AGU PUBLICATIONS

JGR

Journal of Geophysical Research: Solid Earth

RESEARCH ARTICLE
10.1002/2016JB013410

Resonant Ultrasound Spectroscopy studies of Berea sandstone at high temperature

Eric S. Davis[1], Blake T. Sturtevant[1], Dipen N. Sinha[1], and Cristian Pantea[1]

[1]Materials Physics and Applications, MPA-11, Los Alamos National Laboratory, Los Alamos, New Mexico, USA

Key Points:
- Elastic properties of Berea sandstone were studied at high temperatures
- Berea sandstone exhibits anomalous elastic behavior between 385 and 478 K
- Room temperature RUS bulk modulus measurements agree well with literature

Correspondence to:
C. Pantea,
pantea@lanl.gov

Citation:
Davis, E. S., B. T. Sturtevant, D. N. Sinha, and C. Pantea (2016), Resonant Ultrasound Spectroscopy studies of Berea sandstone at high temperature, *J. Geophys. Res. Solid Earth*, *121*, 6401–6410, doi:10.1002/2016JB013410.

Received 27 JUL 2016
Accepted 31 AUG 2016
Accepted article online 4 SEP 2016
Published online 17 SEP 2016

Abstract Resonant Ultrasound Spectroscopy was used to determine the elastic moduli of Berea sandstone from room temperature to 478 K. Sandstone is a common component of oil reservoirs, and the temperature range was chosen to be representative of typical downhole conditions, down to about 8 km. In agreement with previous works, Berea sandstone was found to be relatively soft with a bulk modulus of approximately 6 GPa as compared to 37.5 GPa for α-quartz at room temperature and pressure. It was found that Berea sandstone undergoes a ~17% softening in bulk modulus between room temperature and 385 K, followed by an abnormal behavior of similar stiffening between 385 K and 478 K.

1. Introduction

Understanding the mechanical properties of rocks beneath Earth's surface, at temperatures typically found in oil wells, is of great importance to the oil/gas and geothermal industry. This knowledge has become even more important with the recent rise of hydraulic fracturing (fracking) as a preferred method for oil and gas extraction. Sandstone is commonly found in oil and gas reservoirs [*Slatt*, 2013], and detailed calculations based on the mechanical properties of the reservoir's constituent materials are needed to safely and efficiently extract oil or gas. This requirement creates a great need to determine the elastic properties of the sandstone not only at room temperature but also at higher temperatures to simulate downhole conditions as temperatures quickly rise with increased drilling depth at a rate of approximately 25 K/km [*Finger and Blankenship*, 2010].

Several earlier studies, briefly described here, were performed on sandstones in order to determine their mechanical properties under different conditions of pressures and temperatures. Ulrich and Darling performed a qualitative study on the elastic properties dependence with temperature for Berea sandstone. The temperature range covered was room temperature to about 8 K. They showed the existence of a hysteresis in elastic properties with cooling versus warming and also the presence of an anomalous behavior which indicates that Berea sandstone is softening with decrease in temperature between 200 K and 60 K. [*Ulrich and Darling*, 2001]. Liang et al. discovered that salt rock strength is affected very little by strain rate and that there is a logarithmic relationship between deformation modulus and loading strain rate [*Liang et al.,* 2011]. Ten Cate and Shankland explored slow dynamics in Berea sandstone and found that it has a strong memory of strain history and hysteresis in resonant frequencies with changing strain amplitude [*Ten Cate and Shankland*, 1996]. Costin and Holcomb found that cyclic loading can induce microcrack damage in rocks and cause specimen failure that is inconsistent with results extrapolated from static tests. Additionally, Costin and Holcomb found that high stress can destroy discrete memory in rock specimens and reduce stress cycle hysteresis [*Costin and Holcomb*, 1981]. Rocks, and particularly sandstone, exhibit several unusual elastic responses to stress that include nonclassical attenuation, stress-strain hysteresis, slow dynamics, and high vibrational energy loss due to internal defects [*Johnson et al.,* 1999; *Lebedev*, 2002]. These features, combined with the acoustic nonlinearity of the material that is due to the bond system controlling the elastic properties rather than the grains, result in rock being an extremely difficult material to study mechanically [*Nobili et al.,* 2005]. These materials merit further study as their mechanical behavior has a strong temperature dependence. Several factors, such as temperature, pressure, composition, porosity, and moisture, are known to affect the elastic properties of porous materials [*Zhang and Bentley*, 2003]. Berea sandstone is a relatively soft, porous material that is highly attenuating to sound and attributes most of its mechanical properties to quartz, which is its major constituent. Berea sandstone has a porosity of 13% to 23% and is composed of 93.13% silica, 3.86% alumina, 0.54% ferrous oxide, 0.25% magnesia, 0.11% ferric oxide, and 0.10% calcium oxide (www.bereasandstonecores.com). Berea sandstone exhibits no known temperature-induced phase transitions between room temperature and ~846 K.

Most past studies of Berea sandstone's elastic properties have used pulse-echo or transmit-receive approaches [*Winkler*, 1983; *Green and Wang*, 1994]. Harris and Wang used Differential Acoustic Resonance Spectroscopy which allows for a wide variety of sample shapes and quick sample preparation and works by measuring the resonance shift between a fluid-filled cavity and the same cavity with a sample placed inside. This technique has allowed for very low frequency sound speed measurements on rock samples with highly irregular shapes and extremely small dimensions with results comparable to literature values [*Harris et al.,* 2005; *Wang et al.,* 2012]. Hart and Wang measured the poroelastic moduli of Berea sandstone using static stress-strain measurements under varying pore pressure conditions [*Hart and Wang*, 1995]. Ulrich used Resonant Ultrasound Spectroscopy (RUS) to perform a qualitative study of the behavior of Berea sandstone at low temperatures [*Ulrich and Darling*, 2001], while Ten Cate [*Ten Cate and Shankland*, 1996] and Johnson [*Johnson et al.,* 2004], used a variation of RUS, Nonlinear RUS (NRUS) to investigate its slow dynamics. *Renaud et al.* [2013] used a dynamic acoustoelastic method to investigate the elasticity of dry Berea sandstone as a function of applied low-frequency axial strain.

This paper focuses exclusively on high-temperature effects, using RUS, a technique known to provide elastic constants with high accuracy [*Migliori and Sarrao*, 1997]. The RUS technique is treated exhaustively in *Migliori and Sarrao* [1997], but is described here briefly for completeness. RUS is used to accurately and nondestructively extract the elastic moduli of a small solid object of well-defined geometry using the material's natural mechanical resonances. In RUS, a swept frequency acoustic signal is applied to the sample through a piezoelectric transducer, while the mechanical response is recorded using a second transducer in contact with the sample. This technique can be applied to a wide variety of sample types and geometries with very little material needed and provides the highest accuracy for determination of elastic constants, with typical accuracies of 0.5–1.0% for compressional moduli and 0.2% for shear moduli from fits with a 0.1–0.2% RMS error [*Migliori and Sarrao*, 1997; *Pandey and Schreuer*, 2012; *Liu et al*., 2008; *Sedmák et al.,* 2013]. Additionally, RUS is capable of measurements over a significantly large temperature and pressure range which is important for simulating inner-earth conditions and elucidating effects of changing environment on the mechanical properties of materials.

2. Experimental

The Berea sandstone sample used in our study was cut and prepared into a rectangular parallelepiped with the dimensions $9.13 \times 8.32 \times 6.65\ mm^3$. The small sample size was chosen to avoid low-frequency resonances which would couple to other parts of the experimental apparatus. Small samples have the added advantage that they are effectively isotropic, a feature that is not necessarily true for a larger sedimentary sample [*Sayers et al.,* 1990]. As the largest wavelength used in this study (12.55 mm) is several magnitudes larger than the average grain size of Berea sandstone, isotropy can be assumed for the Berea sample. The sample was mounted between two Boston PiezoOptics, $6 \times 2 \times 3.25$ mm, 1 MHz, 36° Y-cut (*P* wave or longitudinally polarized) LiNbO3 piezoelectric transducers. In theory, RUS assumes free boundary conditions for the sample. Experimentally, this is achieved by using point contacts between the sample and the transducers. Corner mounting of the transducers was attempted to achieve this condition and to reduce noise from transducer contact, but it was found that such a mounting implementation was not only impractical for the environmental conditions in this study but also difficult to achieve from the standpoint of obtaining sufficient acoustic signal through the transducer. Consequently, the transducers were affixed with a high-temperature epoxy (EPO-TEK, TM112) to the 9.13×6.65 mm face parallel to the 9.13 mm side of the sample (Figure 1). The sample/transducer assembly was placed into a small-diameter tube furnace (Blue M) with a proportional integral differential controller (Eurotherm 847) for precise temperature manipulation. The furnace environment initially consisted of ambient air and remained unmodified throughout the experiment except by temperature change. Near-sample temperature was obtained using a type-J thermocouple attached to a data acquisition module (MC USB-TC-AI DAQ, Measurement Computing). RUS spectra were obtained using a vector network analyzer (Bode 100, Omicron Lab) connected to a computer for data acquisition. Prior to data collection, the sample was heated to 478 K for a period of 2 h to thoroughly dry the sample. After this initial baking, the sample and transducers were brought back to room temperature inside the furnace tube with both ends stuffed with quartz wool. The following day, the sample and transducer were heated to 478 K in less than an hour and then cooled to room temperature over a period of approximately 7 h. During sample cooling, the furnace temperature was briefly (~5 min) stabilized every

Figure 1. The $LiNbO_3$ transducers attached to opposing faces of the 9.13 × 6.65 × 8.32 mm Berea sandstone sample using high-temperature epoxy.

5 K so that data could be collected. Each spectrum spanned frequencies between 50 kHz and 170 kHz with 4096 points, and the network analyzer had a source power of 12.0 dBm and an IF bandwidth of 100 Hz. Each sweep took approximately 4 min, during which the furnace temperature was stable to within 1 K.

3. Results

Based on theoretical calculations, the frequency region studied here covers the first 31 resonances for the sample used in this study. In order to reliably determine elastic moduli, it is generally accepted that one must have at least five resonances per elastic modulus [*Migliori and Sarrao*, 1997]. An isotropic polycrystalline sample, such as the one studied here, has two independent elastic moduli, requiring at least 10 resonances to be taken into account.

At each temperature, the RUS spectrum was analyzed using freely available RUS analysis code available at https://nationalmaglab.org/user-facilities/dc-field/dcfield-techniques/resonant-ultrasound-dc. As an example of the procedure used, the room temperature data analysis will be described in the next section.

3.1. Room Temperature

The room temperature RUS spectrum is shown in Figure 2. The quality factor (Q), calculated here as the frequency of a peak divided by its full width at half maximum, ranged from 100 to 250 depending on the resonance being considered. This Q factor is in agreement with that obtained by Winkler et al. which reported a Q of ~140–170 for dry Berea sandstone at low strain amplitudes [*Winkler et al.,* 1979]. Although Berea sandstone is highly attenuating, it can be seen in Figure 2 that the resonant frequencies are readily identified, even with the peak broadening associated with a low Q factor and some overlapping of neighboring peaks. For correct mode identification in Berea sandstone, we used different sets of elastic constants, either from literature [*Remillieux et al.,* 2015; *Shankland et al.,* 1993; *Renaud et al.,* 2013; *Winkler et al.,* 1979; *Sayers et al.,* 1990] or from through-transmission experiments for both compressional and shear waves, performed in our lab. These values provide a reasonable starting guess for forward calculation of the resonant frequencies. Multiple room temperature fittings were performed with a wide variety of Cij values until error minimization between computed and experimental resonances was achieved. Experimental modes corresponding strongly with their calculated room temperature counterparts can then be tracked with temperature as they exhibit only small shifts between successive temperature steps.

Table 1 presents the results obtained from a fit to the room temperature experimental resonance data. The fit was calculated using 14 basis functions. The columns in Table 1 are as follows: (1) the resonance number; (2)

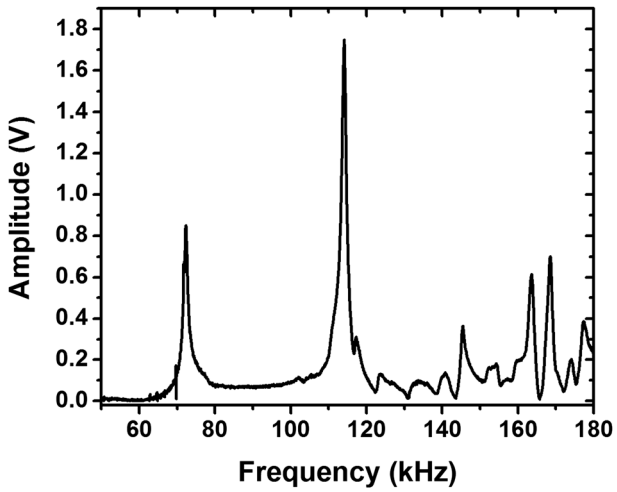

Figure 2. A typical RUS spectrum collected in this study, at room temperature.

the experimental resonance frequencies (f_{ex}); (3) resonance frequencies (f_r) calculated from the fitting software; (4) percent error for each resonance, %err = $(f_r - f_{ex})/f_{ex} \times 100$; (5) a weighting factor, wt, between 0 and 1 that indicates how heavily the fit procedure should consider each resonance (0 means do not consider and 1 means consider fully); (6) mode symmetry (k) as described in Migliori and Sarrao; (7) order (i); and finally, (8) the sensitivity of each resonance frequency to the elastic moduli normalized to unity (df/dC_{11} and df/dC_{44}.)

The root-mean-square (RMS) error of the fit $\left(\sqrt{\sum_n \frac{(f_r - f_{ex})^2}{n}} \times 100\right)$ shown in the table was 0.33%, which gives a high confidence for the calculated values of elastic moduli. As seen in Table 1, two resonances, at

Table 1. Room Temperature RUS Fit of Berea Sandstone

n	f_{ex} (kHz)	f_r (kHz)	%err	wt	k	i	df/dC_{11}	df/dC_{44}
1	72.59	72.85	0.35	1.00	4	1	0.00	1.00
2	96.83	96.91	0.08	1.00	6	2	0.22	0.78
3	100.81	100.49	−0.32	1.00	4	2	0.00	1.00
4	103.40	103.35	−0.05	1.00	7	2	0.32	0.68
5	108.56	108.90	0.32	1.00	3	2	0.04	0.96
6	114.11	113.95	−0.14	1.00	6	3	0.62	0.38
7	117.03	118.28	1.07	0.00	1	2	0.27	0.73
8	120.02	120.05	0.03	1.00	2	2	0.03	0.97
9	122.98	122.19	−0.65	1.00	5	1	0.06	0.94
10	124.51	124.35	−0.13	1.00	8	2	0.04	0.96
11	129.25	128.82	−0.33	1.00	8	3	0.28	0.72
12	131.61	131.16	−0.34	1.00	5	2	0.20	0.80
13	132.88	132.97	0.07	1.00	2	3	0.33	0.67
14	139.59	139.63	0.03	1.00	5	3	0.24	0.76
15	145.32	147.95	1.81	0.00	7	3	0.47	0.53
16	151.75	150.84	−0.60	1.00	1	3	0.51	0.49
17	152.52	152.47	−0.04	1.00	8	4	0.04	0.96
18	154.67	154.15	−0.34	1.00	5	4	0.59	0.41
19	156.80	156.93	0.09	1.00	3	3	0.35	0.65
20	159.09	159.99	0.56	1.00	5	5	0.67	0.33
21	163.73	164.19	0.28	1.00	4	3	0.16	0.84
22	165.76	165.38	−0.23	1.00	6	4	0.24	0.76
23	166.03	166.29	0.16	1.00	2	4	0.05	0.95
24	168.61	169.21	0.36	1.00	1	4	0.10	0.90
25	169.58	169.74	0.10	1.00	7	4	0.14	0.86

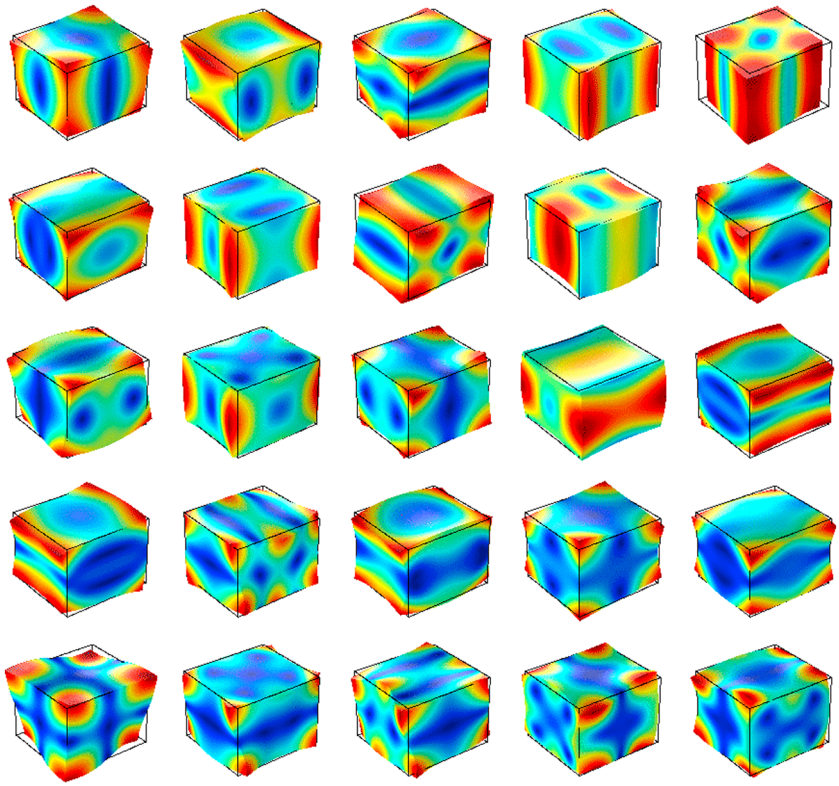

Figure 3. Resonance modes for Berea sandstone at room temperature—modes are in order.

117.03 and 145.32 kHz, were omitted from the calculations. After multiple fitting attempts, these resonances were obvious outliers and could not be fit to better than 1%. Considering that Berea sandstone is a porous material, and the transducers were glued on the sample, it is not unexpected that some resonances will be affected more than others by these artifacts. RUS fits that included anisotropy were also investigated (cubic and hexagonal) but did not lead to significant improvement of the fit or to significant changes in determined elastic moduli. This finding indicates that the earlier stated assumption that the sample is isotropic on these length scales is reasonable.

Once a stable fit was obtained, the room temperature dimensions of the sample were also allowed to vary, resulting in the following dimensions of the sample: $9.05 \times 8.23 \times 6.81$ mm^3. These dimensions are different by about 1–2% compared to our measured values. Due to the porous nature of the material, the corners of the sample are not perfectly sharp. Allowing the dimensions to vary in the fitting routine accounts for this artifact to some extent. Thermal expansion of the sample was accounted for in calculation of the elastic moduli for each temperature step using available thermal expansion data [*Somerton and Selim*, 1961]. The volumetric thermal expansion was estimated as $43.7 \cdot 10^{-6}\,\mathrm{K}^{-1}$ from Figure 3 in the reference above.

The first 25 resonance modes for the sample used in this study are depicted graphically and in order (first left to right and then top to bottom) in Figure 3. The graphical representations are calculated using COMSOL Multiphysics. For each mode, the instantaneous particle displacements are shown using a thermometer color scheme where blue is low (cold) and red is a high value (hot). No correlation between face displacement of poorly fitted modes and the face on which the transducers were mounted was found. This is illustrated by comparing Table 1 to Figure 3 in which poorly fitted modes had a degenerate mode that fit well.

The room temperature values of C_{11} and C_{44} were found to be 12.2 and 4.8 GPa, respectively. From these values and the density ($\rho = 2115$ kg/m^3) determined from the measured mass and the fit dimensions of the sample, the following quantities of interest were calculated: bulk modulus $B = 5.8$ GPa, Young's modulus $E = 11.32$ GPa, Poisson ratio $\nu = 0.17$, compressional sound speed $v_P = 2402$ m/s, shear sound speed $v_S = 1511$ m/s, and $v_P/v_s = 1.59$.

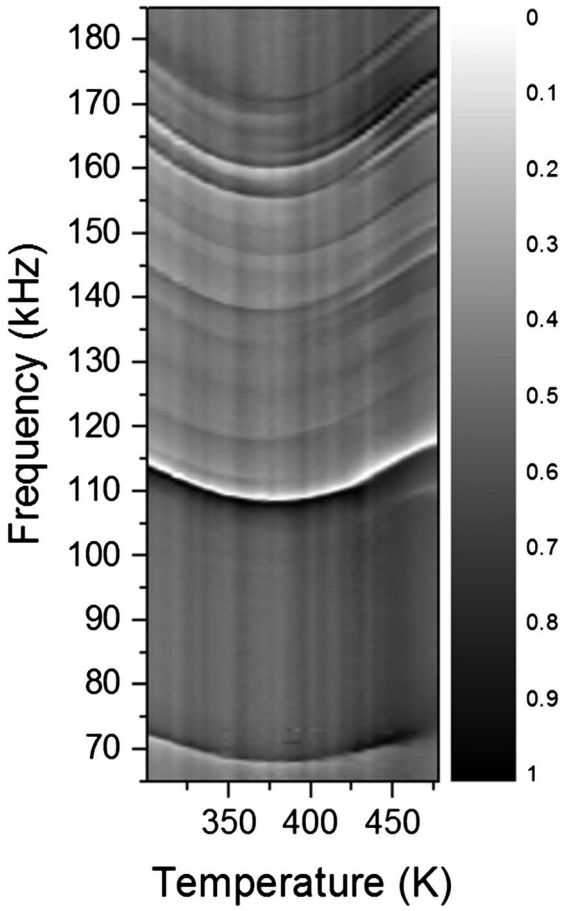

Figure 4. Resonance spectra for each temperature step. The amplitudes are normalized to the highest amplitude at each temperature. Higher amplitudes are designated by darker color.

The room temperature elastic constants C_{11} and C_{44} are within 12% of recently published data on Berea sandstone [*Remillieux et al.,* 2015], which reports $C_{11} = 10.86$ GPa and $C_{44} = 4.24$ GPa. These values lead to similar values for Young's modulus, $E = 10$ GPa, and Poisson's ratio, $\nu = 0.18$. The compressional sound speed is in good agreement with *Shankland et al.* [1993] and *Renaud et al.* [2013] who report values of $v_P = 2380$ m/s and $v_P = 2450$ m/s, respectively. However, the values determined here differ by as much as 50% when compared to Winkler ($v_P = 1930$ m/s) [*Winkler et al.,* 1979] and Sayers ($v_P = 3280$–3600 m/s) [*Sayers et al.,* 1990]. Such differences are common in the sandstone literature and can be attributed to different densities and/or porosities of the samples used in each individual study.

3.2. Temperature Dependence

All spectra versus temperature are plotted in Figure 4. Each spectrum is plotted at its corresponding temperature with darker color indicating higher amplitude. For example, it can be seen that the most prominent resonance in Figure 2, at approximately 115 kHz, corresponds with the darkest line in Figure 4. The strong curvature of the resonance position with respect to temperature shows that Berea sandstone has a very significant resonance shifting with temperature. Two prominent resonant frequencies versus temperature are plotted in Figure 5 and show the characteristically strong dependence of resonant frequency on sample temperature mentioned above. The dependence of resonance frequency on temperature can be separated into two distinct regions. Between room temperature and 385 K, the Berea sandstone exhibits behavior of regular solids, i.e., softening as temperature increases. However, between 385 K and 478 K, the material is found to stiffen with temperature. For example, over the first 100 K, the resonances change by < -400 ppm/K. At ~385 K, the resonances begin increasing at a rate > 400 ppm/K for the final 100 K

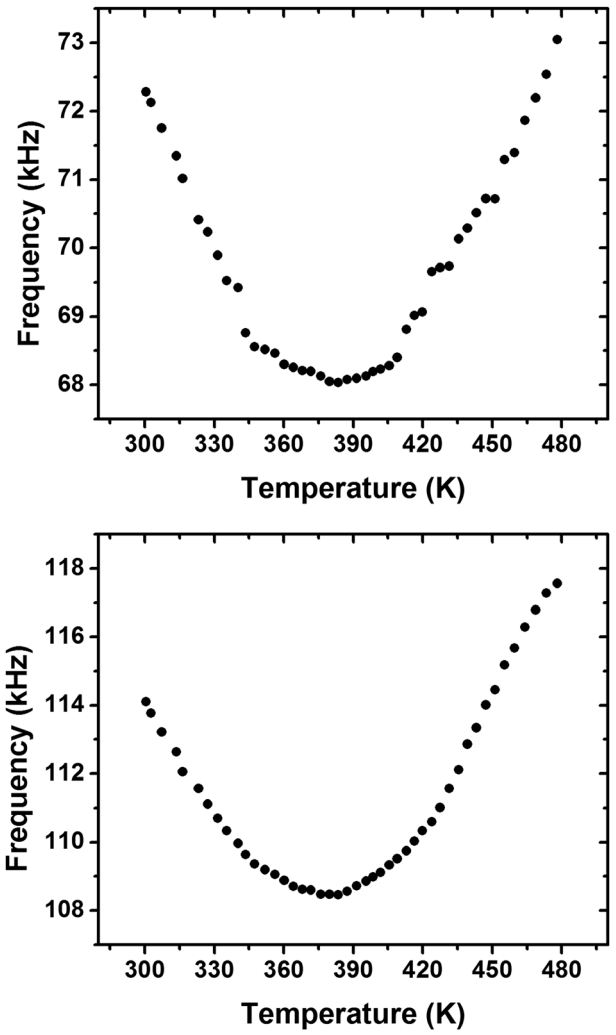

Figure 5. The first and second most prominent resonance frequencies (see Figure 2) plotted versus temperature.

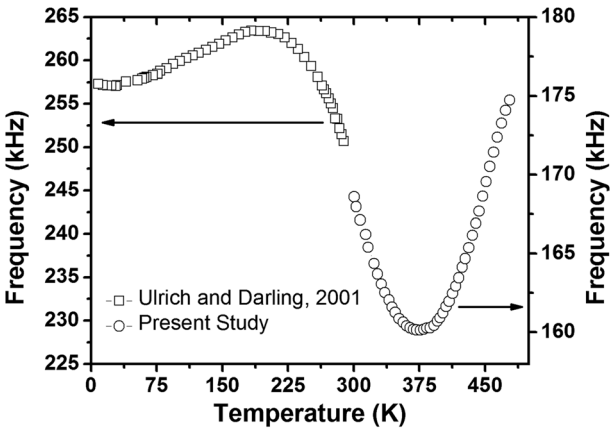

Figure 6. One resonant frequency from this study plotted versus temperature together with frequency data from Ulrich and Darling.

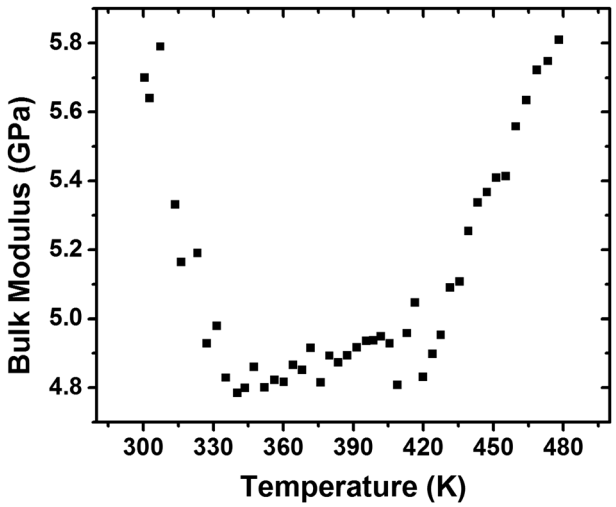

Figure 7. Calculated bulk modulus at each temperature.

considered here. This unexpected behavior was found to be repeatable upon thermal cycling. Additional through-transmission experiments were performed with separate, larger samples (24.80 × 15.86 × 15.86 mm) of Berea sandstone which confirmed the trends seen by these RUS experiments. The results of these experiments are not shown here. Mode stiffening with temperature is unusual and has been observed in few materials [e.g., *Pantea et al.,* 2006; *Wang et al.,* 2015; *Hancock et al.,* 2015].

A qualitative comparison of our data with Ulrich and Darling (Figure 6) shows that Berea softens with temperature between 225 K and 385 K, as is typically found in solids. The anomalous stiffening with temperature can also be observed in the figure in two different temperature regions, $<$200 K and $>$375 K. Figure 7 presents the bulk modulus value $\left(B = C_{11} - \frac{4}{3}C_{44}\right)$ that was calculated from the determined elastic moduli at each temperature. A quantitative analysis of this data reveals an approximately 17% softening with temperature between room temperature and 385 K, followed by an almost equal percentage of stiffening between 385 K and 480 K. By comparing Figure 7 with Figures 4 and 5, it can be seen that the bulk modulus is ~4 times more sensitive to changes in temperature than the individual resonance frequencies. This difference can be largely attributed to the fact that the resonance frequencies include a change not only in material stiffness but also in physical dimension through the coefficients of thermal expansion. Young's modulus and Poisson ratio vary by about 8% and 19%, respectively.

Compressional (C_{11}) and shear (C_{44}) elastic moduli have a similar qualitative temperature dependence and turnover temperature (Figure 8). However, C_{11} can be seen to have a significantly larger quantitative

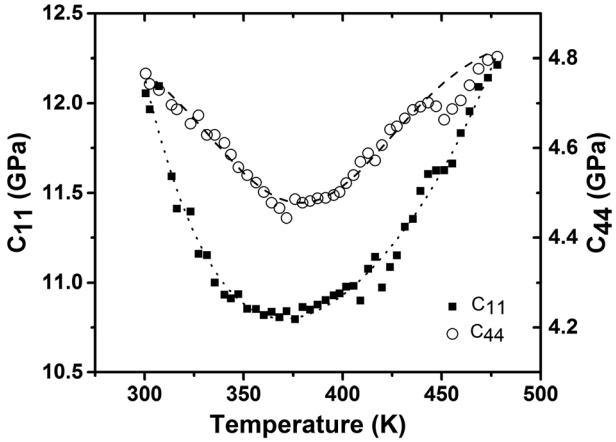

Figure 8. Independent elastic moduli C_{11} and C_{44} plotted versus temperature. Lines are to guide the reade0072's eyes.

temperature dependence, with a ±1000 ppm/K variability compared to C_{44} which has approximately half of that sensitivity or ~ ±600 ppm/K in the same temperature ranges. Considering that Berea sandstone is composed largely of $Si0_2$, it is perhaps interesting to compare the temperature derivatives of the elastic moduli determined here to the well-known values of these quantities for α-quartz [*Bechmann et al.,* 1962]. Around room temperature, the compressional elastic moduli of α-quartz, C_{11} and C_{33}, have first-order temperature coefficients $\left(\frac{1}{C_{xx}}\frac{dC_{xx}}{dT}\right)$ of −49 ppm/K and −160 ppm/K, respectively. These values are remarkably smaller than the −1000 ppm/K for C_{11} mentioned above. The shear moduli for α-quartz have temperature coefficients ranging from −177 ppm/K for C_{44} to +178 ppm/K for C_{66} [*Bechmann et al.,* 1962].

The great span of values for the temperature coefficients for the α-quartz shear moduli likely reflects little more than the fact that it is highly anisotropic (belonging to crystal point group 32), while the Berea sample studied here is assumed isotropic. However, that both compressional moduli of α-quartz are 3–20 times less sensitive to temperature appears to be more significant. This result reinforces the intuitive belief that the mechanical properties of the constituents of a macroscopic composite such as Berea have little bearing on the mechanical properties of the composite, itself.

4. Summary

Resonant Ultrasound Spectroscopy was used for determination of the elastic moduli of dry Berea sandstone, both at room temperature and at high temperatures characteristics to depths of about 8 km. Sample dimensions were chosen to be relatively small, less than 1 cm on every side, in order to avoid complications brought by low frequencies and to minimize the effects of anisotropy. Room temperature data show that Berea sandstone is a very soft material, with a bulk modulus of only 5.8 GPa. It was found that Berea sandstone undergoes a softening between room temperature and 385 K, followed by an abnormal behavior of stiffening between 385 K and 478 K.

Acknowledgments
The authors thank T.J. Ulrich for helpful discussions. This work was partially funded by the U.S. Department of Energy. All data found in section 3 of this paper are available upon request from the corresponding author.

References

Bechmann, R., A. D. Ballato, and T. J. Lukaszek (1962), Higher-order temperature coefficients of the elastic stiffinesses and compliances of alpha-quartz, *Proc. IRE*, *50*(8), 1812–1822, doi:10.1109/JRPROC.1962.288222.

Costin, L. S., and D. J. Holcomb (1981), Time-dependent failure of rock under cyclic loading, *Tectonophysics*, *79*(3), 279–296, doi:10.1016/0040-1951(81)90117-7.

Finger, J., and D. Blankenship (2010), *Handbook of Best Practices for Geothermal Drilling*, Sandia Natl. Lab., Albuquerque, N. M.

Green, D. H., and H. F. Wang (1994), Shear wave velocity and attenuation from pulse-echo studies of Berea sandstone, *J. Geophys. Res.*, *99*, 11,755–11,763, doi:10.1029/94JB00506.

Hancock, J. C., K. W. Chapman, G. J. Halder, C. R. Morelock, B. S. Kaplan, L. C. Gallington, A. Bongiorno, C. Han, S. Zhou, and A. P. Wilkinson (2015), Large negative thermal expansion and anomalous behavior on compression in cubic ReO_3-type $A^{II}B^{IV}F_6$: $CaZrF_6$ and $CaHfF_6$, *Chem. Mater.*, doi:10.1021/acs.chemmater.5b00662.

Harris, J. M., Y. Quan, and C. Xu (2005), Differential acoustical resonance spectroscopy: An experimental method for estimating acoustic attenuation of porous media, SEG Technical Program Expanded Abstracts 2005, pp. 1569–1572, doi:10.1190/1.2147992.

Hart, D. J., and H. F. Wang (1995), Laboratory measurements of a complete set of poroelastic moduli for Berea sandstone and Indiana limestone, *J. Geophys. Res.*, *100*, 17,741–17,751, doi:10.1029/95JB01242.

Johnson, P. A., R. A. Guyer, and L. A. Ostrovsky (1999), A nonlinear mesoscopic elastic class of materials, *AIP Conf. Proc.*, *524*, 291–294, doi:10.1121/1.427349.

Johnson, P. A., B. Zinszner, P. Rasolofosaon, F. Cohen-Tenoudji, and K. Van Den Abeele (2004), Dynamic measurements of the nonlinear elastic parameter α in rock under varying conditions, *J. Geophys. Res.*, *109*, B02202, doi:10.1029/2002JB002038.

Lebedev, A. V. (2002), Method of linear prediction in the ultrasonic spectroscopy of rock, *Acoust. Phys.*, *48*(3), 339–346, doi:10.1134/1.1478120.

Liang, W. G., Y. S. Zhao, S. G. Xu, and M. B. Dusseault (2011), Effect of strain rate on the mechanical properties of salt rock, *Int. J. Rock Mech. Min. Sci.*, *48*(1), 161–167, doi:10.1016/j.ijrmms.2010.06.012.

Liu, Y., H. Wu, C. T. Liu, Z. Zhang, and V. Keppens (2008), Physical factors controlling the ductility of bulk metallic glasses, *Appl. Phys. Lett.*, *93*(15), 151915, doi:10.1063/1.2998410.

Migliori, A., and J. L. Sarrao (1997), *Resonant Ultrasound Spectroscopy: Applications to Physics, Materials Measurements, and Nondestructive Evaluation*, Wiley-Interscience, New York.

Nobili, M., M. Scalerandi, and P. P. Delsanto (2005), Temperature dependence of the elastic properties of hysteretic materials, *Mater. Sci. Forum*, *480*, 573–578, doi:10.4028/www.scientific.net/MSF.480-481.573.

Pandey, C. S., and J. Schreuer (2012), Elastic and piezoelectric constants of tourmaline single crystals at non-ambient temperatures determined by resonant ultrasound spectroscopy, *J. Appl. Phys.*, *111*(1), 013516, doi:10.1063/1.3673820.

Pantea, C., A. Migliori, P. B. Littlewood, Y. Zhao, H. Ledbetter, J. C. Lashley, T. Kimura, J. Van Duijin, and G. R. Kowach (2006), Pressure-induced elastic softening of monocrystalline zirconium tungstate at 300 K, *Phys. Rev. B*, *73*, 214118, doi:10.1103/PhysRevB.73.214118.

Remillieux, M. C., T. J. Ulrich, C. Payan, J. Rivière, C. R. Lake, and P.-Y. Le Bas (2015), Resonant ultrasound spectroscopy for materials with high damping and samples of arbitrary geometry, *J. Geophys. Res. Solid Earth*, *120*, 4898–4916, doi:10.1002/2015JB011932.

Renaud, G., J. Rivière, P.-Y. Le Bas, and P. A. Johnson (2013), Hysteretic nonlinear elasticity of Berea sandstone at low-vibrational strain revealed by dynamic acousto-elastic testing, *Geophys. Res. Lett.*, *40*, 715–719, doi:10.1002/grl.50150.

Sayers, C. M., J. G. Van Munster, and M. S. King (1990), Stress-induced ultrasonic anisotrophy in Berea sandstone, *Int. J. Rock Mech. Min. Sci. Geomech. Abstr.*, *27*(5), 429–436, doi:10.1016/0148-9062(90)92715-Q.

Sedmák, P., H. Seiner, P. Sedlák, M. Landa, R. Mušálek, and J. Matějíček (2013), Application of resonant ultrasound spectroscopy to determine elastic constants of plasma-sprayed coatings with high internal friction, *Surf. Coat. Technol.*, *232*, 747–757, doi:10.1016/j.surfcoat.2013.06.091.

Shankland, T. J., P. A. Johnson, and T. M. Hopson (1993), Elastic wave attenuation and velocity of Berea sandstone measured in the frequency domain, *Geophys. Res. Lett.*, *20*, 391–394, doi:10.1029/92GL02758.

Slatt, R. M. (2013), *Stratigraphic Reservoir Characterization for Petroleum Geologists, Geophysicists, and Engineers*, *Dev. in Pet. Sci.*, vol. 61, Elsevier, Kidlington, U. K.

Somerton, W. H., and M. A. Selim (1961), Additional thermal data for porous rocks—Thermal expansion and heat of reaction, *Soc. Pet. Eng. J.*, doi:10.2118/1613-G.

Ten Cate, J. A., and T. J. Shankland (1996), Slow dynamics in the nonlinear elastic response of Berea sandstone, *Geophys. Res. Lett.*, *23*, 3019–3022, doi:10.1029/96GL02884.

Ulrich, T. J., and T. W. Darling (2001), Observation of anomalous elastic behavior in rock at low temperatures, *Geophys. Res. Lett.*, *28*, 2293–2296, doi:10.1029/2000GL012480.

Wang, L., C. Wang, Y. Sun, K. Shi, S. Deng, H. Lu, P. Hu, and X. Zhang (2015), Metal fluorides, a new family of negative thermal expansion materials, *J. Materiomics*, doi:10.1016/j.jmat.2015.02.001.

Wang, S. X., J. G. Zhao, Z. H. Li, J. M. Harris, and Y. Quan (2012), Differential acoustic resonance spectroscopy for the acoustic measurement of small and irregular samples in the low frequency range, *J. Geophys. Res.*, *117*, B06203, doi:10.1029/2011JB008808.

Winkler, K., A. Nur, and M. Gladwin (1979), Friction and seismic attenuation in rocks, *Nature*, *277*, 528–531, doi:10.1038/277528a0.

Winkler, K. W. (1983), Frequency dependent ultrasonic properties of high-porosity sandstones, *J. Geophys. Res.*, *88*, 9493–9499, doi:10.1029/JB088iB11p09493.

Zhang, J. J., and L. R. Bentley (2003), Pore geometry and elastic moduli in sandstones, CREWES, Univ. of Calgary.